



OPEN ACCESS

EDITED BY

Hsiuying Wang,
National Yang Ming Chiao Tung University,
Taiwan

REVIEWED BY

Hui Jan Tan,
National University of Malaysia, Malaysia
Pan Liu,
The Central Hospital of Shaoyang, China

*CORRESPONDENCE

Kang Wang
✉ fcwangk1@zju.edu.cn
Peng Xu
✉ xupeng@uestc.edu.cn
Fali Li
✉ fali.li@uestc.edu.cn

†These authors have contributed equally to this work and share first authorship

RECEIVED 24 February 2023

ACCEPTED 10 July 2023

PUBLISHED 20 July 2023

CITATION

Wu D, Jiang L, He R, Chen B, Yao D, Wang K, Xu P and Li F (2023) Brain rhythmic abnormalities in convalescent patients with anti-NMDA receptor encephalitis: a resting-state EEG study.
Front. Neurol. 14:1163772.
doi: 10.3389/fneur.2023.1163772

COPYRIGHT

© 2023 Wu, Jiang, He, Chen, Yao, Wang, Xu and Li. This is an open-access article distributed under the terms of the [Creative Commons Attribution License \(CC BY\)](https://creativecommons.org/licenses/by/4.0/). The use, distribution or reproduction in other forums is permitted, provided the original author(s) and the copyright owner(s) are credited and that the original publication in this journal is cited, in accordance with accepted academic practice. No use, distribution or reproduction is permitted which does not comply with these terms.

Brain rhythmic abnormalities in convalescent patients with anti-NMDA receptor encephalitis: a resting-state EEG study

Dengchang Wu^{1†}, Lin Jiang^{2,3†}, Runyang He^{2,3}, Baodan Chen^{2,3}, Dezhong Yao^{2,3,4,5}, Kang Wang^{1*}, Peng Xu^{2,3,4,6*} and Fali Li^{2,3,4*}

¹Department of Neurology, The First Affiliated Hospital, School of Medicine, Zhejiang University, Hangzhou, China, ²The Clinical Hospital of Chengdu Brain Science Institute, MOE Key Lab for Neuroinformation, University of Electronic Science and Technology of China, Chengdu, China, ³School of Life Science and Technology, Center for Information in BioMedicine, University of Electronic Science and Technology of China, Chengdu, China, ⁴Research Unit of NeuroInformation, Chinese Academy of Medical Sciences, Chengdu, China, ⁵School of Electrical Engineering, Zhengzhou University, Zhengzhou, China, ⁶Radiation Oncology Key Laboratory of Sichuan Province, Chengdu, China

Objective: Anti-N-methyl-D-aspartate receptor encephalitis (anti-NMDARE) is autoimmune encephalitis with a characteristic neuropsychiatric syndrome and persistent cognition deficits even after clinical remission. The objective of this study was to uncover the potential noninvasive and quantified biomarkers related to residual brain distortions in convalescent anti-NMDARE patients.

Methods: Based on resting-state electroencephalograms (EEG), both power spectral density (PSD) and brain network analysis were performed to disclose the persistent distortions of brain rhythms in these patients. Potential biomarkers were then established to distinguish convalescent patients from healthy controls.

Results: Oppositely configured spatial patterns in PSD and network architecture within specific rhythms were identified, as the hyperactivated PSD spanning the middle and posterior regions obstructs the inter-regional information interactions in patients and thereby leads to attenuated frontoparietal and frontotemporal connectivity. Additionally, the EEG indexes within delta and theta rhythms were further clarified to be objective biomarkers that facilitated the noninvasive recognition of convalescent anti-NMDARE patients from healthy populations.

Conclusion: Current findings contributed to understanding the persistent and residual pathological states in convalescent anti-NMDARE patients, as well as informing clinical decisions of prognosis evaluation.

KEYWORDS

anti-NMDAR encephalitis, EEG, power spectral density, brain network, clinical assessment

1. Introduction

As the most frequent human autoimmune encephalitis, anti-N-methyl-D-aspartate receptor encephalitis (anti-NMDARE) is characterized by diverse psychiatric and neurological features, such as memory impairment and psychosis (1, 2). In clinical practice, in addition to the evaluation from experienced physicians, the detection of IgG antibodies against the GluN1 subunit of the receptor in the serum and cerebrospinal fluid (CSF) has

long been the golden criterion for anti-NMDARE diagnosis (3, 4). Whereas the follow-up of antibody titers was not perfectly correlated with the disease course (5), antibodies may still be recognized in the CSF and serum of patients even after clinical recovery (6). Although 75% of the patients have a favorable outcome with substantial recovery (7), persistent deficits in memory, attention, and executive functioning (8–12) still occur.

The diagnosis based on magnetic resonance imaging can be normal or nonspecific (13), providing limited diagnostic and prognostic value. Given a quantitative and specific method is lacking to guide noninvasive and precise evaluation for this disease, other objective tests seem to be imperative to track therapy with a specific biomarker of brain activity, as well as to potentially monitor the treatment course. In this regard, the registration of spontaneous activity by electroencephalogram (EEG) seems to be a practical way, which has been extensively incorporated into clinical evaluations for its inexpensive, non-invasive, and widely available nature. EEG is abnormal in almost anti-NMDARE patients during the acute phase, showing disorganized background activity (1, 14), which seems to be useful in the clinical diagnosis of anti-NMDARE (15). Whereas the majority of previous EEG research concentrates on the raw signal manifestations during the acute stage (16, 17), further exploring the EEG biomarkers may have the potential for rapid diagnosis and prognostic evaluation of anti-NMDARE within varying courses. More importantly, scalp EEG provides a noninvasive and objective tool for studying the brain (dys) function (18, 19); thus, EEG is believed to be capable to assess the brain deficits of anti-NMDARE patients even during convalescence, as well as to differentiate convalescent patients from healthy controls (HCs).

Hence, based on our previous studies which verified the negative effect of anti-NMDARE on the patient's brain at different therapeutic stages, such as hyperactivated regional activity in hippocampus/parahippocampus and worse memory retrieval performance, etc. at the post-acute stage (20, 21), in the current study, quantitative EEG analysis was carried out to probe the role of the brain rhythmic alteration in the course of the anti-NMDARE. Therein, we expected that the distinguished resting-state EEG metrics could be regarded as the biomarkers to quantify the therapy of anti-NMDARE and provide potential clinical guidance for the future follow-up of these patients. To achieve this, resting-state EEG datasets of anti-NMDARE patients during the convalescence and gender- and age-matched HCs were collected. Theoretically, cortical oscillations play essential roles in a wide range of neural activities, especially since changes in spectral power by neurocognitive disease within specific rhythms have been widely reported (22, 23). In addition, other than isolated brain regions, the network that helps reveal information propagation among spatially distributed regions (24) was also considered. As such, power spectral density (PSD) which provides valuable information on regional power characteristics of spontaneous activities was first investigated, and brain network analysis was performed to explore the intrinsic rhythmic difference between anti-NMDARE patients and HCs, which is expected to provide potential biomarkers for distinguishing convalescent anti-NMDARE patients from HCs, as well as tracking the therapeutic effect in future studies.

2. Materials and methods

2.1. Patients

Under the approval of the Ethics Committee of the First Affiliated Hospital, Zhejiang University School of Medicine, 36 right-handed participants, including 18 convalescent anti-NMDARE patients (15 females, age 27.22 ± 12.28 , Table 1) and 18 gender- and age-matched HCs (15 females, age 27.56 ± 11.51), were enrolled. Herein, all patients were diagnosed according to the detection of IgG antibodies for NMDA receptors and other typical clinical symptoms (1, 4). And in addition to the history of neurologic or psychiatric disorders, we also excluded the patient with abnormal lesions in magnetic resonance imaging (MRI) scans to exclude the possible coexisting conditions. Concerning the HC, these gender- and age-matched participants had been also confirmed to have no history of psychological or neurological disorders. Before resting-state EEG monitoring, all participants had fully understood the experimental protocol and signed the written informed consent.

2.2. Clinical status

Patients can be diagnosed as stronger positive, positive, weak positive, and negative based on the antibody titers. And the modified Rankin Scale (mRS) was also measured to evaluate the neurological outcome per patient. In essence, patients are considered fully recovered (i.e., mRS=0) if they can return to work; patients are considered mildly deficient (i.e., mRS=1 or 2) if they can return to most daily activities and keep stable for more than 2 months; in other cases, patients were considered seriously deficient. Herein, all patients enrolled were considered in convalescence, as the antibody titer level was negative and the maximal mRS score was 1 according to the medical records (Table 1). In the meantime, we tested 8–18 antibodies of autoimmune encephalitis in the CSF and serum for all patients, and all of them showed only NMDA-IgG positive.

2.3. EEG data recording

The resting-state EEG was collected by 32-channel digital video-EEG systems (Nicolet v32, Natus Neurology Incorporated, Middleton, WI, USA). All electrodes were positioned in compliance with the international 10/20 system. The impedance of each electrode was kept below 5 k Ω , and electrode AFz was set as the reference. EEG was band-pass filtered at 0.01–100 Hz and sampled at 500 Hz.

2.4. EEG analysis

The analytical procedures are depicted in Figure 1 and consist of EEG pre-processing, PSD analysis, network analysis, and classification. The pre-processing aims to acquire artifact-free segments, and the following analyses will further explore the disease-induced aberrant patterns of resting-state rhythmic activity in convalescent patients. The details are described below.

TABLE 1 Clinical and demographic information of the patients.

Participant	Sex	Age	NMDAR-IgG onset	NMDAR-IgG recovery phase	mRS onset	mRS recovery
Patient 1	F	50	1:32	1:1	5	1
Patient 2	F	32	1:32	1:1	5	0
Patient 3	F	15	1:32	1:1	5	0
Patient 4	F	22	1:32	1:10	5	0
Patient 5	F	25	1:32	1:1	2	0
Patient 6	F	20	1:32	1:10	3	0
Patient 7	F	24	1:32	1:1	5	0
Patient 8	M	46	1:3.2	0	5	1
Patient 9	M	28	1:32	1:10	5	0
Patient 10	M	58	1:32	1:1	5	0
Patient 11	F	22	1:32	1:10	5	0
Patient 12	F	15	1:10	1:1	5	0
Patient 13	F	17	1:10	1:1	5	0
Patient 14	F	29	1:32	1:1	5	0
Patient 15	F	19	1:32	1:10	5	0
Patient 16	F	21	1:10	1:1	5	0
Patient 17	F	29	1:32	1:10	5	0
Patient 18	F	18	1:32	1:1	5	0

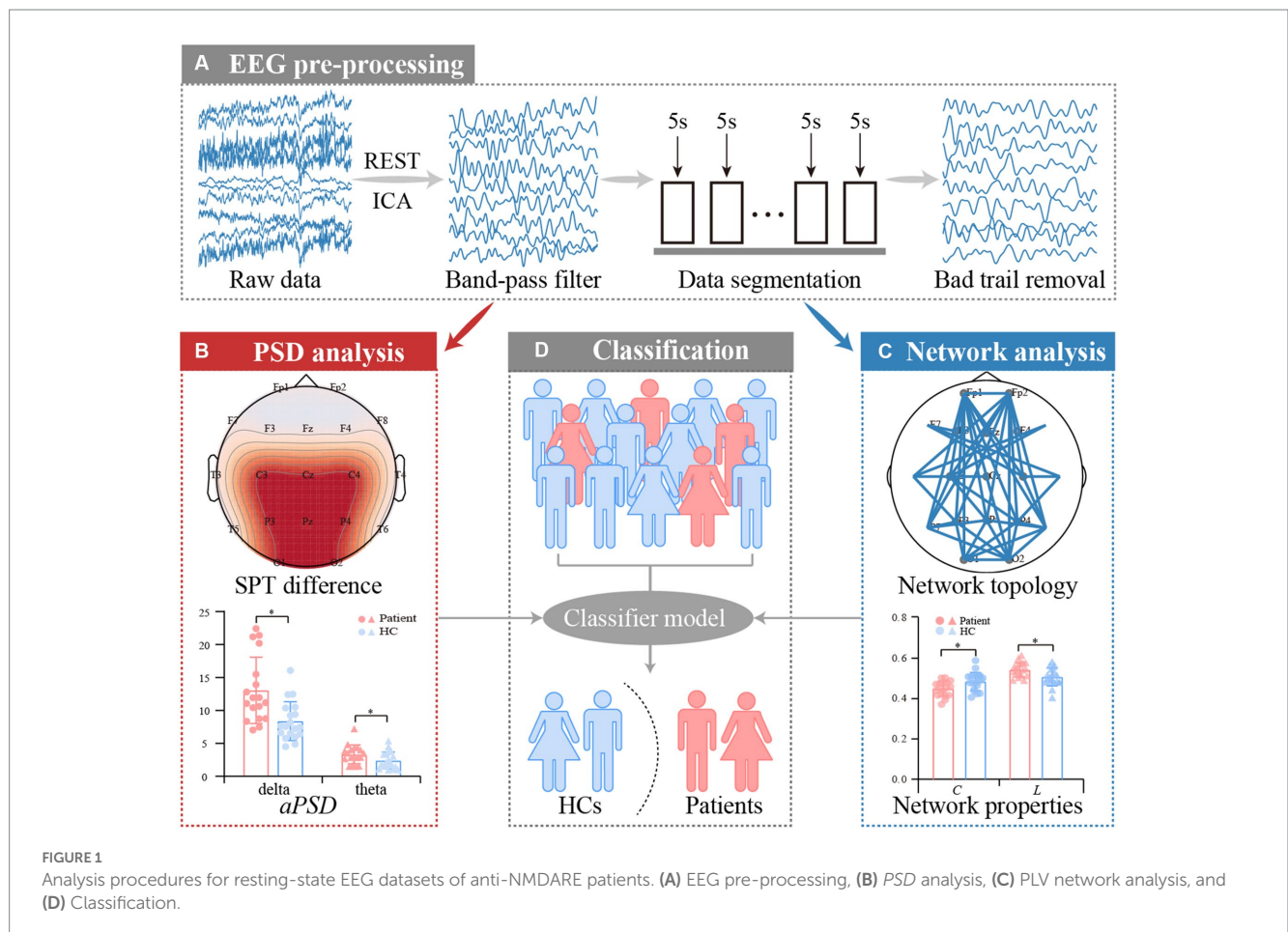


FIGURE 1 Analysis procedures for resting-state EEG datasets of anti-NMDARE patients. (A) EEG pre-processing, (B) PSD analysis, (C) PLV network analysis, and (D) Classification.

2.4.1. EEG pre-processing

The EEG datasets were first re-referenced to a neutral reference by the Reference Electrode Standardization Technique (REST) (25, 26). Thereafter, multiple standard procedures including the independent component analysis (27), 0.5–45 Hz bandpass filtering, 5 s data segmenting, and ±90 μV artifacts removal were carried out accordingly.

2.4.2. Power spectral density

For each participant, the remaining segments after preprocessing were trial-averaged, and the corresponding PSD was then calculated by Welch's method within a frequency range of interest f , i.e., delta (0.5–4 Hz), theta (4–8 Hz), alpha (8–13 Hz), beta (13–30 Hz), and gamma (30–45 Hz). Subsequently, the scalp power topographies (SPTs) per band were plotted, and the absolute PSD (*aPSD*) was also evaluated. Specifically, based on the PSD of each frequency bin f , the *aPSD* value was defined and calculated as,

$$aPSD_{\xi}(\sigma) = \sum_{f=f_1}^{f_2} PSD(f), \text{ if } \begin{cases} \sigma = \text{delta} & [f_1, f_2] = [0.5, 4] \\ \sigma = \text{theta} & [f_1, f_2] = [4, 8] \\ \sigma = \text{alpha} & [f_1, f_2] = [8, 13] \\ \sigma = \text{beta} & [f_1, f_2] = [13, 30] \\ \sigma = \text{gamma} & [f_1, f_2] = [30, 45] \end{cases} \text{ , then } \quad (1)$$

where ξ denotes the types of anti-NMDARE patients or HCs.

2.4.3. PLV network

Based on the preprocessed EEG segments, the phase-locking value (PLV) was then applied to construct related functional brain networks (28). First, to assess the instantaneous phases, $\varphi_u(t)$ and $\varphi_v(t)$, of signals $u(t)$ and $v(t)$, the Hilbert transform (*HT*) was applied to establish the analytical signal $H(t)$,

$$\begin{aligned} H_u &= u(t) + iHT_u(t) \\ H_v &= v(t) + iHT_v(t) \end{aligned} \quad (2)$$

where $HT_u(t)$ and $HT_v(t)$ indicate the *HT* of the two signals and can be formulated as,

$$\begin{aligned} HT_u &= \frac{1}{\pi} P.V. \int_{-\infty}^{\infty} \frac{u(t')}{t-t'} dt' \\ HT_v &= \frac{1}{\pi} P.V. \int_{-\infty}^{\infty} \frac{v(t')}{t-t'} dt' \end{aligned} \quad (3)$$

where the *P.V.* is the Cauchy principal value. Consequently, the phases of the analytical signals, $\varphi_u(t)$ and $\varphi_v(t)$, are defined as,

$$\begin{aligned} \varphi_u &= \arctan \frac{HT_u(t)}{u(t)} \\ \varphi_v &= \arctan \frac{HT_v(t)}{v(t)} \end{aligned} \quad (4)$$

Then, the PLV can be calculated as,

$$w^{PLV} = \left| \frac{1}{N} \sum_{j=0}^{N-1} e^{i(\varphi_u(j\Delta t) - \varphi_v(j\Delta t))} \right| \quad (5)$$

where N and t indicate the sample number and the time point, respectively. Δt denotes the sampling period, j is the j -th sample point, and w^{PLV} represents the connection weight.

For each interested band, the weighted adjacency matrixes were formed to index the information exchange among all electrodes, and then matrixes of all segments were averaged to obtain the final matrix for each participant.

2.4.4. Network properties

The characteristic path length (L) and clustering coefficient (C) were two essential network indicators reflecting the global and local information processing ability of brain networks, respectively, which can be computed by the brain connectivity toolbox (BCT, <http://www.nitrc.org/projects/bct/>) (29) as,

$$C = \frac{1}{M} \sum_{i \in \theta} \frac{\sum_{j, l \in \theta} (w_{ij} w_{il} w_{jl})^{1/3}}{\sum_{j \in \theta} w_{ij} (\sum_{j \in \theta} w_{ij} - 1)} \quad (6)$$

$$L = \frac{1}{M} \sum_{i \in \theta} L_i = \frac{1}{N} \sum_{i \in \theta} \frac{\sum_{j \in \theta, j \neq i} d_{ij}}{N-1} \quad (7)$$

where w_{ij} and d_{ij} represent the connection strength and the shortest weighted path length between node i and j , respectively. θ and M indicate the set of all nodes and the node number of the network, respectively.

2.4.5. Statistical analysis

Within each interested band, the independent sample t -test was statistically performed to quantify potential relationships, i.e., the differences in *SPT*, *aPSD*, network topologies, and properties, between the convalescent patients and HCs. Then, a false discovery rate (FDR) was performed to correct the p -values, in which the corrected significant p -values were verified to have at least $p < 0.01$.

2.4.6. Classification between the anti-NMDARE patients and HCs

Considering that *PSD* and functional networks reflect different aspects of spontaneous brain operation, both might provide complementary and comprehensive information for discrimination between anti-NMDARE patients and HCs. In this work, in addition to *aPSD* and network properties, the discriminative spatial pattern of the network (SPN) was also calculated (30). Hence, using the SPN features, *aPSD*, and network properties, we further classified the convalescent patients from HCs by the support vector machine (SVM) with leave-one-out cross-validation (LOOCV) strategy (31). Thereafter, to evaluate the classification performance, the accuracy, specificity, and sensitivity were calculated as,

$$Accuracy = \frac{n_{PAs} + n_{HCs}}{N_{PAs} + N_{HCs}} \times 100\% \tag{8}$$

$$Sensitivity = \frac{n_{PAs}}{N_{PAs}} \times 100\% \tag{9}$$

$$Specificity = \frac{n_{HCs}}{N_{HCs}} \times 100\% \tag{10}$$

where n_{PAs} and n_{HCs} represent the correct number of anti-NMDARE patients and HCs, respectively. N_{PAs} and N_{HCs} represent the total number of anti-NMDARE patients and HCs, respectively.

3. Results

3.1. Differential scalp power topographies

Figure 2A exhibits the SPT patterns between convalescent patients and HCs in the five bands. Generally, in contrast to HCs, the EEG power of the convalescent patients experienced a significant enhancement within delta and theta bands ($p < 0.01$, FDR corrected), which were distributed in extensive frontal, parietal, and occipital regions. However, no differences were captured for the other three bands. Given the prominent variation of delta and theta SPT, the

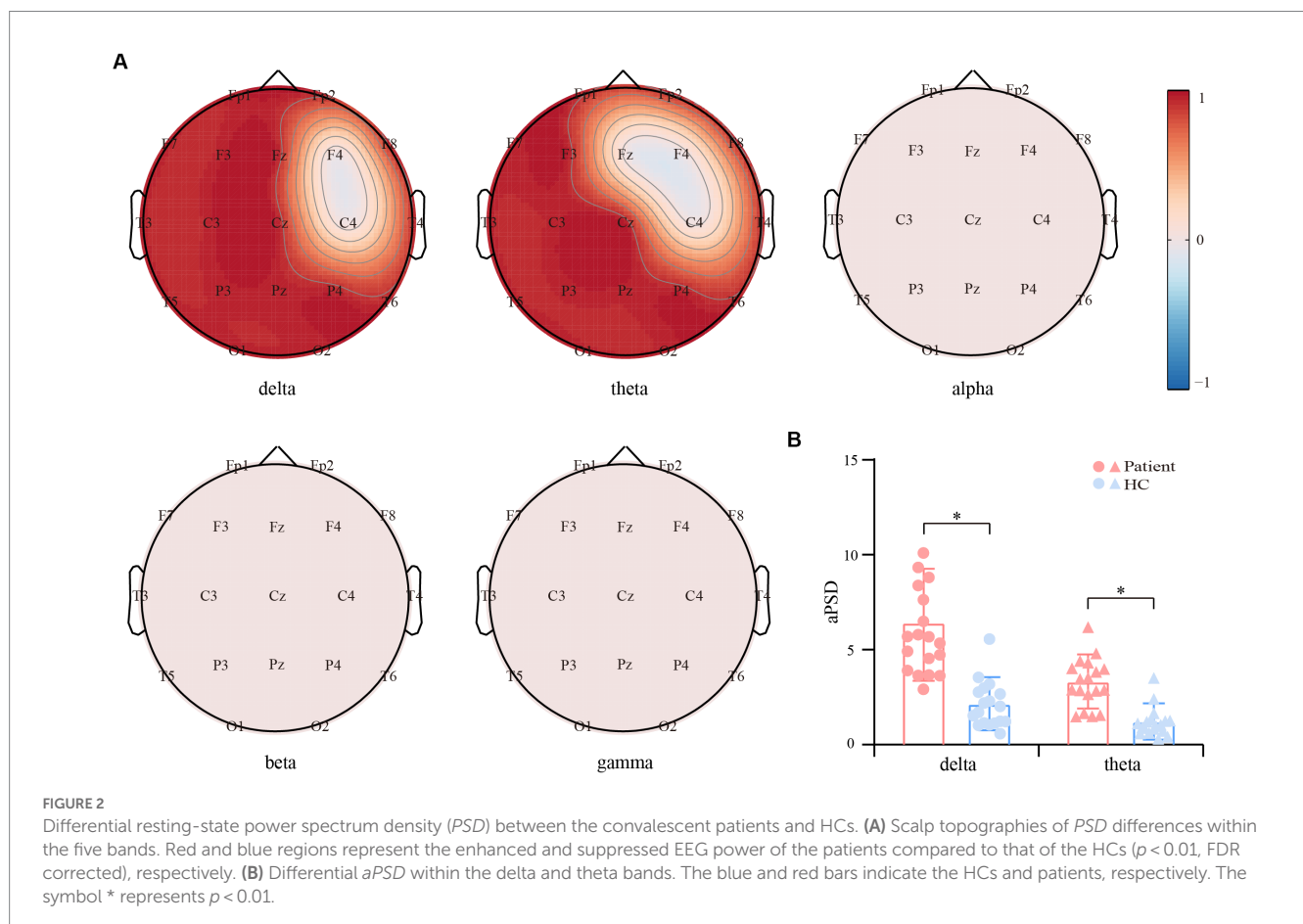
grand-averaged *aPSD* across all electrodes was calculated and statistically compared between both groups. As shown in Figure 2B, within both rhythms, the convalescent patients exhibit significantly increased *aPSD*, when compared to that of the HCs ($p < 0.01$).

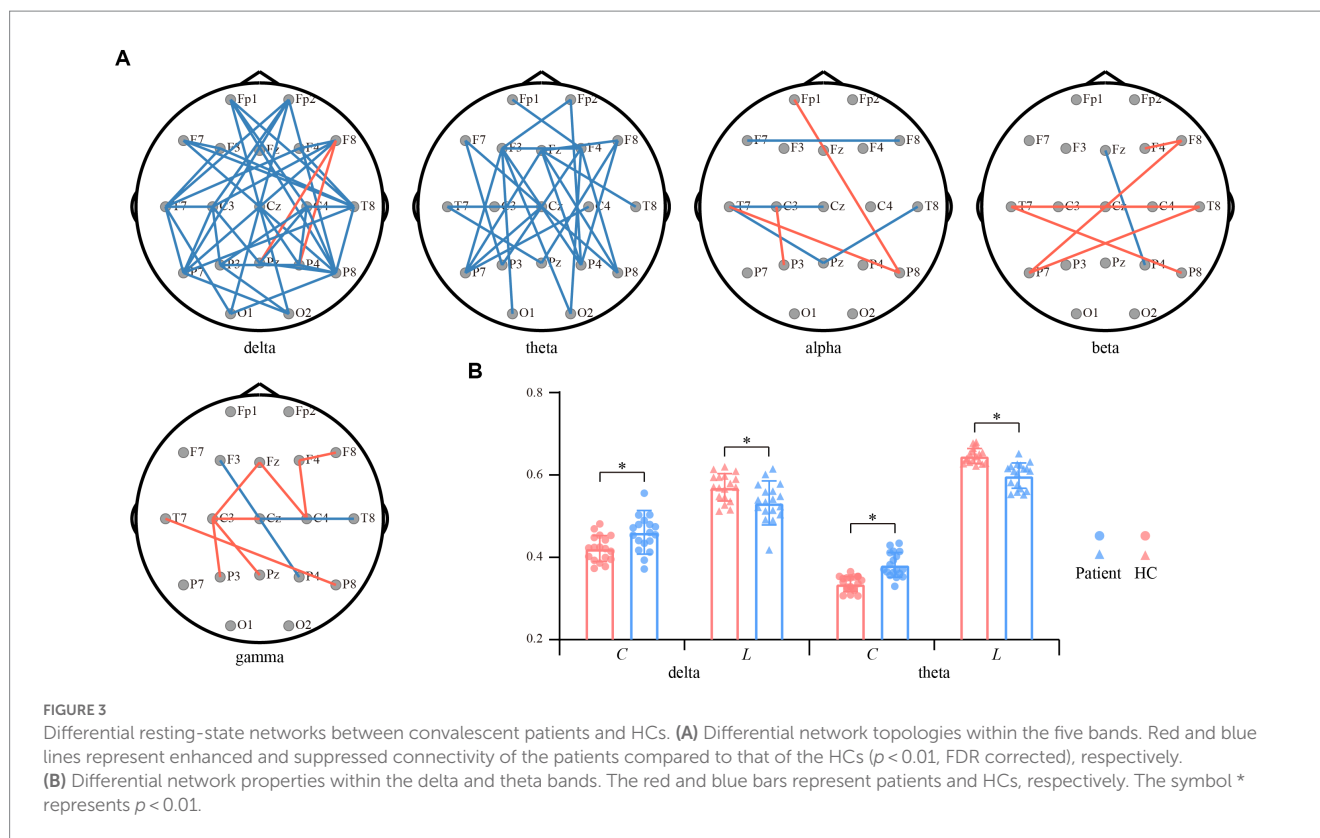
3.2. Differential functional brain networks

In contrast to the *PSD*, functional network architectures for both interest bands (i.e., the delta and theta) show the opposite reorganized patterns (Figure 3A). Specifically, in the delta and theta bands, the PLV couplings spanning the frontal, temporal, and parietal lobes were attenuated for the convalescent anti-NMDARE patients in contrast to that of the HCs ($p < 0.01$, FDR corrected). Whereas, within the other bands, there only existed small portions of connections that exhibited significant differences. Figure 3B further shows the network properties of both bands, in which, the decreased *C* and longer *L* of the patients deviating from the HCs were found ($p < 0.01$), which coincided with the significantly reduced connections in Figure 3A.

3.3. Categorization into anti-NMDARE patients and HCs

Given the significant differences identified above, we then investigated if these indexes could be regarded as biomarkers for anti-NMDARE identification. Thereinto, to capture the spatial





network topologies, SPN was first applied to extract the inherent topological information. Notably, as exhibited in Figure 4, brain regions with significantly different network connections were highlighted with larger coefficients. Finally, by merging the *aPSD*, network metrics, and SPN features, we performed the classification of convalescent anti-NMDARE patients from HCs. Results show that an accuracy of 97.22%, specificity of 94.44%, and sensitivity of 100% were achieved by SVM. Namely, only one out of 36 subjects were falsely classified into the opposite groups, indicating a good classification performance.

4. Discussion

Up to now, the objective and quantified evaluation of brain deficits in convalescent anti-NMDARE patients has not been achieved accurately and noninvasively. Developing specific and objective biological markers is of great significance for the prognosis evaluation and discharge of this disease. Given the diagnostic value of EEG has received increasing attention in anti-NMDARE, herein, resting-state EEG of convalescent anti-NMDARE patients was recorded during the hospitalization and based on which, *SPTs* and network patterns were investigated to identify the reorganized and distorted brain rhythms, as well as develop potential biomarkers for distinguishing convalescent patients from HCs.

In this study, the rhythm-specific *SPTs* that reflect the regional distortion of EEG power in convalescent anti-NMDARE patients are given in Figure 2A. Concretely, within both delta and theta rhythms, the larger rhythmic power, as well as the increasing *aPSD*,

were found in patients and centralized mainly in the middle and posterior brain regions. It appeared that patients with anti-NMDARE may experience disturbances in the brain rhythm even after undergoing treatment and recovering, especially for the delta and theta rhythms. Of note, the current results are globally in line with previous evidence showing that most patients have extensive EEG abnormalities characterized by generalized or focal slow delta-theta activity (32), which might be associated with a possible autoimmune etiology (33). As reported, delta oscillation is essential for the normal functioning of the human brain, and the increasing delta power has been widely documented in developmental disorders and pathological conditions, e.g., schizophrenia (34) and Alzheimer's disease (35). Concerning the anti-NMDARE, the enhanced delta power in the NMDA-receptor antibodies positive model across a wide range of time-constant fluctuations has also been reported (36), while the weaker delta power thereby indicates a recovery in patients with encephalitis (37). Additionally, a higher delta peak is found to be associated with poorer clinical outcomes and thus indicates anti-NMDAR-mediated synaptic dysfunction (38). Considering theta activity is regarded as a credible EEG indicator of normal brain functions including attention and memory (39), and delta activity is involved in the integration of cerebral activity with homeostatic processes (40), the distortions of both rhythmic powers may thereby implicate the persistent and residual pathological states such as anhedonia or reward deficiency (40) in anti-NMDARE patients even after clinical recovery.

In contrast to the increasing EEG power, the attenuated network interactions that can quantify the dysfunctional resource allocations in these patients are depicted in Figure 3. In essence, previous studies

have identified extensive impaired network connections in anti-NMDARE patients during the acute stage, including the visual, lateral-temporal, frontal–parietal, and sensorimotor networks (41, 42). Although these patients recruited in the current study had good therapeutical outcomes during convalescence, the inter-regional couplings within both delta and theta bands were still attenuated, in contrast to that of the HCs (Figure 3A). As proved in previous studies, the distorted frontal–parietal connections may relate to the psychotic symptoms (43), coinciding with the psychiatric model which relies on the frontal–parietal connectivity and NMDAR regulation (44). Additionally, abnormal frontal connectivity might also be associated with disrupted executive function in anti-NMDARE patients (45), while the attenuated occipital connectivity was assumed to be accompanied by reduced visual acuity that correlated with disease severity (46). Collectively, current observations may suggest the residual expression of NMDARs across the extensive brain regions and emphasize its persistent detrimental influence in convalescent patients.

Another possible interesting issue was about the opposite alterations between EEG power and functional networks. This is an expected result as the hyperactivated EEG power across extensive brain regions (Figure 2A) in turn obstructs the inter-regional information interaction, thereby resulting in the reduced functional connectivity in Figure 3A. Further, the disturbed network topologies were also quantitatively measured by the changing network properties of C and L (Figure 3B). As network properties directly measure the network efficiency (47), smaller C and longer L consistently illustrate the decreasing information processing capacity and efficiency of the

brain, and might also index the impaired brain efficiency in convalescent anti-NMDARE patients. As such, the human brain works in a relatively balanced way to effectively process information, the rhythmic alterations in patients were governed by the need for information processing, which may reveal the underlying pathomechanism of the anti-NMDARE.

Thereafter, specifically investigating in Figure 4, we observed that the SPN filters can directly capture the topological differences between the two groups, as brain regions with differentiated interregional information interactions were marked with larger coefficients. In the meantime, given the significant rhythmic alterations in patients found above, features of EEG power and network patterns were further fused to distinguish convalescent anti-NMDARE patients from HCs. As illustrated, the performance further confirmed that these EEG features were feasible and might be reliable biomarkers to quantify the residual brain deficits in convalescent patients, as an accuracy of 97.22% (specificity of 94.44% and sensitivity of 100%) was achieved. These consistently reminded us that the resting-state EEG metrics might be the potential biomarker for future prognostic evaluation of convalescent anti-NMDARE patients, which could be the future direction for the following studies.

One possible limitation would be that the current analyses concentrated on the patients in the recovery phase, leaving the acute stage unmined. Therefore, in future works, patients in both the acute and recovery phases would be recruited, along with their EEG being collected. By performing related analyses, particularly the contrast between the two phases, the findings derived from our current study would be further validated.

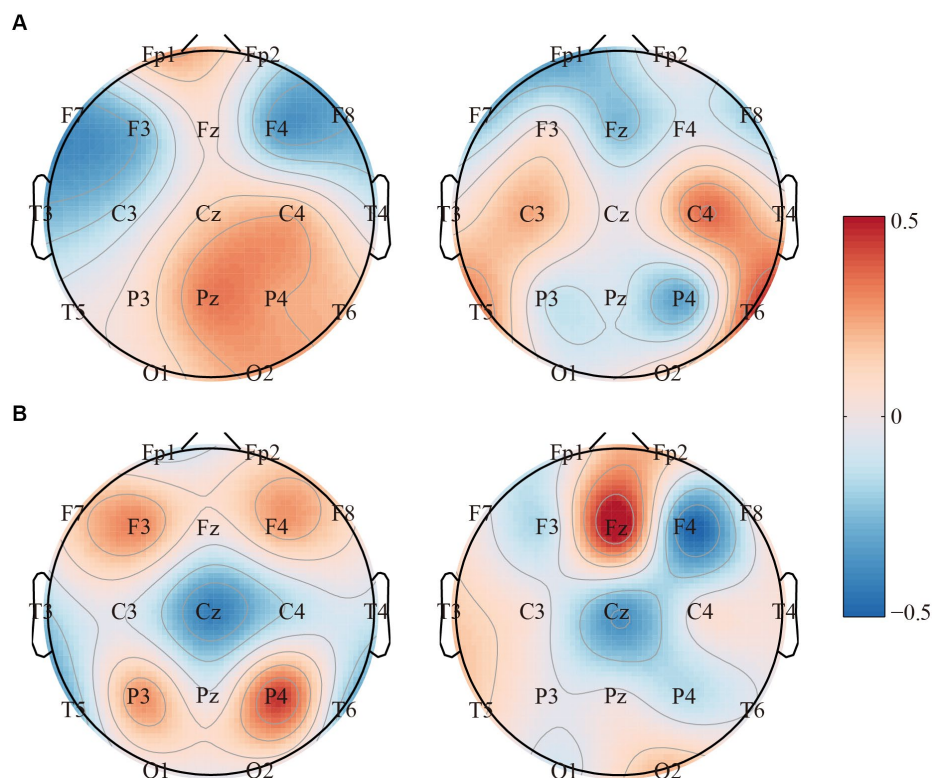


FIGURE 4
The topographies of the SPN filters for the (A) delta band and (B) theta band, respectively.

5. Conclusion

This study investigated the rhythm-specific distortions of EEG power and network topologies in anti-NMDARE patients even after clinical recovery. We found oppositely configured patterns of EEG power and networks in the delta and theta bands, as the hyperactivated brain power obstructs the inter-regional information interactions in patients and further leads to attenuated frontoparietal and frontotemporal couplings. Importantly, merging EEG power and network features of delta and theta bands helped reliably differentiate the convalescent patients from HCs. Taken together, our observations provide new insights into the neural mechanism underlying the residual brain deficits in convalescent anti-NMDARE patients, and the distinguished resting-state EEG metrics are also expected to serve as the biomarkers for quantifying the therapy of anti-NMDARE, as well as providing potential clinical guidance for the future follow-up of these patients.

Data availability statement

The raw data supporting the conclusions of this article will be made available by the authors, without undue reservation.

Ethics statement

The studies involving human participants were reviewed and approved by the Ethics Committee of the First Affiliated Hospital, Zhejiang University School of Medicine. The patients/participants provided their written informed consent to participate in this study.

References

- Dalmau J, Lancaster E, Martinez-Hernandez E, Rosenfeld MR, Balice-Gordon R. Clinical experience and laboratory investigations in patients with anti-NMDAR encephalitis. *Lancet Neurol.* (2011) 10:63–74. doi: 10.1016/S1474-4422(10)70253-2
- Dalmau J, Tüzün E, Wu HY, Masjuan J, Rossi JE, Voloschin A, et al. Paraneoplastic anti-N-methyl-D-aspartate receptor encephalitis associated with ovarian teratoma. *Ann Neurol.* (2007) 61:25–36. doi: 10.1002/ana.21050
- Brooks J, Yarbrough ML, Bucelli RC, Day GS. Testing for N-methyl-D-aspartate receptor autoantibodies in clinical practice. *Can J Neurol Sci.* (2020) 47:69–76. doi: 10.1017/cjn.2019.305
- Graus F, Titulaer MJ, Balu R, Benseler S, Bien CG, Cellucci T, et al. A clinical approach to diagnosis of autoimmune encephalitis. *Lancet Neurol.* (2016) 15:391–404. doi: 10.1016/S1474-4422(15)00401-9
- Gresa-Arribas N, Titulaer MJ, Torrents A, Aguilar E, McCracken L, Leypoldt F, et al. Antibody titres at diagnosis and during follow-up of anti-NMDA receptor encephalitis: a retrospective study. *Lancet Neurol.* (2014) 13:167–77. doi: 10.1016/S1474-4422(13)70282-5
- Hansen H-C, Klingbeil C, Dalmau J, Li W, Weißbrich B, Wandinger K-P. Persistent intrathecal antibody synthesis 15 years after recovering from anti-N-methyl-D-aspartate receptor encephalitis. *JAMA Neurol.* (2013) 70:117–9. doi: 10.1001/jamaneurol.2013.585
- Titulaer MJ, McCracken L, Gabilondo I, Armangué T, Glaser C, Iizuka T, et al. Treatment and prognostic factors for long-term outcome in patients with anti-NMDA receptor encephalitis: an observational cohort study. *Lancet Neurol.* (2013) 12:157–65. doi: 10.1016/S1474-4422(12)70310-1
- de Bruijn MAAM, Aarsen FK, van Oosterhout M, van der Knoop M, Catsman-Berrevoets CE, Schreurs MW, et al. Long-term neuropsychological outcome following pediatric anti-NMDAR encephalitis. *Neurology.* (2018) 90:e1997–2005. doi: 10.1212/WNL.0000000000005605
- Gordon-Lipkin E, Yeshokumar AK, Saylor D, Arenivas A, Probasco JC. Comparative outcomes in children and adults with anti-N-methyl-D-aspartate (anti-

Author contributions

DW and KW designed the study and wrote the protocol. LJ and BC managed the literature searches. LJ and RH performed the data analyses. LJ, BC, and RH undertook the statistical analysis. LJ and DW wrote the first draft of the manuscript, which was critically revised by FL, PX, KW, and DY. All authors contributed to and have approved the final manuscript.

Funding

This work was supported by the National Natural Science Foundation of China (#U19A2082 and #62103085) and the Zhejiang Provincial Natural Science Foundation of China (#LY19H090020).

Conflict of interest

The authors declare that the research was conducted in the absence of any commercial or financial relationships that could be construed as a potential conflict of interest.

Publisher's note

All claims expressed in this article are solely those of the authors and do not necessarily represent those of their affiliated organizations, or those of the publisher, the editors and the reviewers. Any product that may be evaluated in this article, or claim that may be made by its manufacturer, is not guaranteed or endorsed by the publisher.

- NMDA) receptor encephalitis. *J Child Neurol.* (2017) 32:930–5. doi: 10.1177/0883073817720340
- McKeon GL, Robinson GA, Ryan AE, Blum S, Gillis D, Finke C, et al. Cognitive outcomes following anti-N-methyl-D-aspartate receptor encephalitis: a systematic review. *J Clin Exp Neuropsychol.* (2018) 40:234–52. doi: 10.1080/13803395.2017.1329408
 - McKeon GL, Scott JG, Spooner DM, Ryan AE, Blum S, Gillis D, et al. Cognitive and social functioning deficits after anti-N-methyl-D-aspartate receptor encephalitis: an exploratory case series. *J Int Neuropsychol Soc.* (2016) 22:828–38. doi: 10.1017/S1355617716000679
 - Yeshokumar AK, Gordon-Lipkin E, Arenivas A, Cohen J, Venkatesan A, Saylor D, et al. Neurobehavioral outcomes in autoimmune encephalitis. *J Neuroimmunol.* (2017) 312:8–14. doi: 10.1016/j.jneuroim.2017.08.010
 - Wang J, Wang K, Wu D, Liang H, Zheng X, Luo B. Extreme delta brush guides to the diagnosis of anti-NMDAR encephalitis. *J Neurol Sci.* (2015) 353:81–3. doi: 10.1016/j.jns.2015.04.009
 - Scheer S, John RM. Anti-N-methyl-D-aspartate receptor encephalitis in children and adolescents. *J Pediatr Health Care.* (2016) 30:347–58. doi: 10.1016/j.pedhc.2015.09.004
 - da Silva-Júnior FP, Castro LHM, Andrade JQ, Bastos CG, Moreira CH, Valério RMF, et al. Serial and prolonged EEG monitoring in anti-N-methyl-d-aspartate receptor encephalitis. *Clin Neurophysiol.* (2014) 125:1541–4. doi: 10.1016/j.clinph.2014.01.001
 - Limotai C, Denlertchaikul C, Saraya AW, Jirasakuldej S. Predictive values and specificity of electroencephalographic findings in autoimmune encephalitis diagnosis. *Epilepsy Behav.* (2018) 84:29–36. doi: 10.1016/j.yebeh.2018.04.007
 - Zhang Y, Liu G, Di Jiang M, Li LP, Su YY. Analysis of electroencephalogram characteristics of anti-NMDA receptor encephalitis patients in China. *Clin Neurophysiol.* (2017) 128:1227–33. doi: 10.1016/j.clinph.2017.04.015
 - Li F, Wang J, Liao Y, Yi C, Jiang Y, Si Y, et al. Differentiation of schizophrenia by combining the spatial EEG brain network patterns of rest and task P300. *IEEE Trans Neural Syst Rehabil Eng.* (2019) 27:594–602. doi: 10.1109/TNSRE.2019.2900725

19. Zhang X, Jiang Y, Zhang S, Li F, Pei C, He G, et al. Correlation analysis of EEG brain network with modulated acoustic stimulation for chronic tinnitus patients. *IEEE Trans Neural Syst Rehabil Eng.* (2020) 29:156–62. doi: 10.1109/TNSRE.2020.3039555
20. Chen Z, Zhou J, Wu D, Ji C, Luo B, Wang K. Altered executive control network connectivity in anti-NMDA receptor encephalitis. *Ann Clin Transl Neurol.* (2021) 9:30–40. doi: 10.1002/acn3.51487
21. Wang K, Wu D, Ji C, Luo B, Wang C, Chen Z. Abnormal brain activation during verbal memory encoding in Postacute anti-N-methyl-D-aspartate receptor encephalitis. *Brain Connect.* (2021) 12:660–9. doi: 10.1089/brain.2021.0046
22. Benwell CS, Davila-Pérez P, Fried PJ, Jones RN, Travison TG, Santarnecchi E, et al. EEG spectral power abnormalities and their relationship with cognitive dysfunction in patients with Alzheimer's disease and type 2 diabetes. *Neurobiol Aging.* (2020) 85:83–95. doi: 10.1016/j.neurobiolaging.2019.10.004
23. Roh JH, Park MH, Ko D, Park K-W, Lee D-H, Han C, et al. Region and frequency specific changes of spectral power in Alzheimer's disease and mild cognitive impairment. *Clin Neurophysiol.* (2011) 122:2169–76. doi: 10.1016/j.clinph.2011.03.023
24. Li F, Liu T, Wang F, Li H, Gong D, Zhang R, et al. Relationships between the resting-state network and the P3: evidence from a scalp EEG study. *Sci Rep.* (2015) 5:15129. doi: 10.1038/Srep15129
25. Dong L, Li F, Liu Q, Wen X, Lai Y, Xu P, et al. MATLAB toolboxes for reference electrode standardization technique (REST) of scalp EEG. *Front Neurosci.* (2017) 11:601. doi: 10.3389/fnins.2017.00601
26. Yao D. A method to standardize a reference of scalp EEG recordings to a point at infinity. *Physiol Meas.* (2001) 22:693–711. doi: 10.1088/0967-3334/22/4/305
27. Cardoso J-F. Infomax and maximum likelihood for blind source separation. *IEEE Signal Process Lett.* (1997) 4:112–4. doi: 10.1109/97.566704
28. Sakkalis V. Review of advanced techniques for the estimation of brain connectivity measured with EEG/MEG. *Comput Biol Med.* (2011) 41:1110–7. doi: 10.1016/j.combiomed.2011.06.020
29. Rubinov M, Sporns O. Complex network measures of brain connectivity: uses and interpretations. *NeuroImage.* (2010) 52:1059–69. doi: 10.1016/j.neuroimage.2009.10.003
30. Xu P, Xiong X, Xue Q, Li P, Zhang R, Wang Z, et al. Differentiating between psychogenic nonepileptic seizures and epilepsy based on common spatial pattern of weighted EEG resting networks. *IEEE Trans Biomed Eng.* (2014) 61:1747–55. doi: 10.1109/TBME.2014.2305159
31. Zeng L-L, Shen H, Liu L, Wang L, Li B, Fang P, et al. Identifying major depression using whole-brain functional connectivity: a multivariate pattern analysis. *Brain.* (2012) 135:1498–507. doi: 10.1093/brain/awb059
32. Gable MS, Sheriff H, Dalmau J, Tilley DH, Glaser CA. The frequency of autoimmune N-methyl-D-aspartate receptor encephalitis surpasses that of individual viral etiologies in young individuals enrolled in the California encephalitis project. *Clin Infect Dis.* (2012) 54:899–904. doi: 10.1093/cid/cir1038
33. Baysal-Kirac L, Tuzun E, Altindag E, Ekizoglu E, Kinay D, Bilgic B, et al. Are there any specific EEG findings in autoimmune epilepsies? *Clin EEG Neurosci.* (2016) 47:224–34. doi: 10.1177/1550059415595907
34. Bates AT, Kiehl KA, Laurens KR, Liddle PF. Low-frequency EEG oscillations associated with information processing in schizophrenia. *Schizophr Res.* (2009) 115:222–30. doi: 10.1016/j.schres.2009.09.036
35. Babiloni C, Ferri R, Binetti G, Vecchio F, Frisoni GB, Lanuzza B, et al. Directionality of EEG synchronization in Alzheimer's disease subjects. *Neurobiol Aging.* (2009) 30:93–102. doi: 10.1016/j.neurobiolaging.2007.05.007
36. Rosch RE, Wright S, Cooray G, Papadopoulou M, Goyal S, Lim M, et al. NMDA-receptor antibodies alter cortical microcircuit dynamics. *Proc Natl Acad Sci U S A.* (2018) 115:E9916–25. doi: 10.1073/pnas.1804846115
37. Harmony T. The functional significance of delta oscillations in cognitive processing. *Front Integr Neurosci.* (2013) 7:83. doi: 10.3389/fnint.2013.00083
38. Blackman G, Kumar K, Hanrahan JG, Dalrymple A, Mullatti N, Moran N, et al. Quantitative EEG as a prognostic tool in suspected anti-N-methyl-D-aspartate receptor antibody encephalitis. *J Clin Neurophysiol.* (2021) 40:160–4. doi: 10.1097/WNP.0000000000000877
39. Mitchell DJ, McNaughton N, Flanagan D, Kirk IJ. Frontal-midline theta from the perspective of hippocampal "theta". *Prog Neurobiol.* (2008) 86:156–85. doi: 10.1016/j.neurobio.2008.09.005
40. Knyazev GG. EEG delta oscillations as a correlate of basic homeostatic and motivational processes. *Neurosci Biobehav Rev.* (2012) 36:677–95. doi: 10.1016/j.neubiorev.2011.10.002
41. Finke C, Kopp UA, Scheel M, Pech LM, Soemmer C, Schlichting J, et al. Functional and structural brain changes in anti-N-methyl-D-aspartate receptor encephalitis. *Ann Neurol.* (2013) 74:284–96. doi: 10.1002/ana.23932
42. Peer M, Prüss H, Ben-Dayan I, Paul F, Arzy S, Finke C. Functional connectivity of large-scale brain networks in patients with anti-NMDA receptor encephalitis: an observational study. *Lancet Psychiatry.* (2017) 4:768–74. doi: 10.1016/S2215-0366(17)30330-9
43. Anticevic A, Gancsos M, Murray JD, Repovs G, Driesen NR, Ennis DJ, et al. NMDA receptor function in large-scale anticorrelated neural systems with implications for cognition and schizophrenia. *Proc Natl Acad Sci U S A.* (2012) 109:16720–5. doi: 10.1073/pnas.1208494109
44. Stephan KE, Friston KJ, Frith CD. Dysconnection in schizophrenia: from abnormal synaptic plasticity to failures of self-monitoring. *Schizophr Bull.* (2009) 35:509–27. doi: 10.1093/schbul/sbn176
45. Finke C, Kopp UA, Prüss H, Dalmau J, Wandinger K-P, Ploner CJ. Cognitive deficits following anti-NMDA receptor encephalitis. *J Neurol Neurosurg Psychiatry.* (2012) 83:195–8. doi: 10.1136/jnnp-2011-300411
46. Brandt AU, Oberwahrenbrock T, Mikolajczak J, Zimmermann H, Prüss H, Paul F, et al. Visual dysfunction, but not retinal thinning, following anti-NMDA receptor encephalitis. *Neurol-Neuroimmunol Neuroinflammation.* (2016) 3:e198. doi: 10.1212/NXI.0000000000000198
47. Si Y, Li F, Li F, Tu J, Yi C, Tao Q, et al. The growing from adolescence to adulthood influences the decision strategy to unfair situations. *IEEE Trans Cogn Dev Syst.* (2020) 13:586–92. doi: 10.1109/TCDS.2020.2981512